Journal of Low Temperature Physics, Vol. 11, Nos. 5/6, 1973

The Kapitza Thermal Boundary Resistance*

R. E. Peterson and A. C. Anderson

Department of Physics and Materials Research Laboratory
University of Illinois, Urbana, Illinois

(Received September 1972; revised November 30, 1972)

A theory of the Kapitza thermal boundary resistance has been developed which includes not only the scattering of phonons at the interface between two different materials, but also the scattering of phonons within either material near the interface. The theory is shown to be in good agreement with present measurements on solid–solid contacts as well as with previously published low-temperature data on the contact between liquid helium and copper.

1. INTRODUCTION

In initially attempting to analyze the data presented below concerning the thermal boundary resistance between two solids, we found that neither the well-known acoustic mismatch model[1] nor the blackbody (phonon radiation limit) model[2] were compatible with our data. At this same time Anderson and Johnson[3] observed that the magnitude of the Kapitza resistance between liquid ^{3}He and Cu seemed to be dominated by the quantity of strain within the Cu but near the interface. This suggested to the present authors that the attenuation or scattering of phonons near the interface may be the missing factor in understanding thermal transport across a solid–solid boundary. Calculations based on this assumption were then shown to give surprisingly good agreement not only for solid–solid contacts,[4] but also for He–solid interfaces.[5] It is the purpose of the present paper to discuss these calculations, to examine their relationship to previous theories, and to test the results against new as well as published experimental data. The general lack of agreement between experiment and previous theories of the thermal boundary resistance has been well documented in several recent review papers[6–10] and will not be repeated here.

*This work was supported in part by the Advanced Research Projects Agency under Contract HC 15-67-C-0221 and the National Science Foundation Grant GH 33634. Based on a Ph.D. dissertation submitted by R. E. Peterson to the University of Illinois.

© 1973 Plenum Publishing Corporation, 227 West 17th Street, New York, N.Y. 10011.

The term Kapitza resistance has often been associated with the thermal boundary resistance at an interface, this in honor of the first individual to observe and study the phenomenon at a He–Cu boundary.[11] Objections are frequently raised to the application of the term Kapitza resistance to solid–solid interfaces, perhaps in the belief that different physical processes are responsible for the temperature discontinuity at a He–Solid boundary vs. a solid–solid boundary. It is occasionally suggested that the term Kapitza resistance not be used at all since the phrase thermal boundary resistance is much more descriptive of the phenomenon. On the other hand, the term Kapitza resistance has also been employed to emphasize that reference was being made to the thermal resistance occurring at the intimate interface between two homogeneous materials. This excludes the thermal impedance contributed, for example, by a strained layer,[12] a layer of dirt, or film boiling.

Having indicated that there are differences of opinion on proper terminology, we will use in the following pages the symbol R_B to represent the thermal impedance occurring at the interface between two homogeneous materials at least one of which is nonmetallic. R_B will have the units of $\text{cm}^2 \cdot \text{K/W}$. Hence R_B is normalized to a unit area of the interface.

2. THEORY

The basic physical process causing R_B is conceptually simple. Since we assume that one of the materials is a dielectric, energy is carried across the boundary by phonons. A thermal impedance occurs because any phonon incident on the boundary has a certain probability of being reflected due to the discontinuity in acoustic properties.

Consider the energy flux across the interface between two semiinfinite isotropic nonmetallic solids. The only energy carriers at temperatures below 1 K are acoustic phonons with a dispersion relation $\omega = c_{ij}k$, where c_{ij} is the velocity of the jth mode in material i, ω is the angular frequency, and k is the magnitude of the wave vector. At low temperatures the Debye approximation is adequate so the energy density $E(\omega)$ at frequency ω for the jth mode in material i is

$$E_{ij}(\omega)\,d\omega = (\hbar\omega^3\,d\omega)[2\pi^2(e^{\hbar\omega/k_bT} - 1)c_{ij}^3]^{-1} \tag{1}$$

where k_b is the Boltzmann constant and $\hbar$ is the Planck constant divided by 2π. The total energy which crosses the interface per unit time and per unit area from material 1 is then

$$\dot{Q}_{1\to 2} = \frac{1}{2}\sum_j \int_0^{\omega_D} \int_0^{\pi/2} E_{1j}(\omega)w_{1j}(\theta_0)c_{1j}\cos\theta_0 \sin\theta_0\,d\theta_0\,d\omega \tag{2}$$

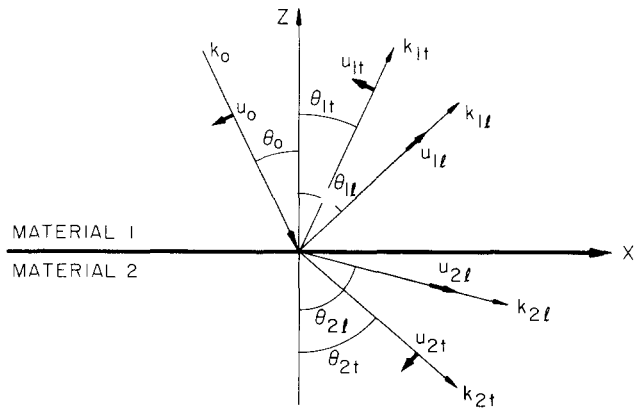

Fig. 1. Reflection and refraction of a transverse wave polarized in the plane of incidence. (0) Incident wave; (1) reflected wave; (2) refracted wave; (l) longitudinal wave; (t) transverse wave. Similar figures could be drawn for the incident longitudinal mode and for the transverse mode polarized perpendicular to the plane of incidence.

where $w_{1j}(\theta_0)$ is the transmission probability, that is, the fraction of energy transmitted to material 2 due to an acoustic wave of mode j incident on the interface from material 1 at an angle θ_0 defined in Fig. 1. We assume for the present that $w_{1j}(\theta_0)$ is independent of frequency. The validity of this assumption and the calculations of w_{1j} are primary topics of the attenuated phonon theory developed below. Performing the frequency integration in the low-temperature approximation gives

$$\dot{Q}_{1\to 2} = \sum_j (\pi^2 k_b^2 T_1^4 / 60\hbar^3 c_{1j}^2) \int_0^1 w_{1j}(\theta_0) \cos\theta_0 \, d(\cos\theta_0) \tag{3}$$

We call $2\int_0^1 w_{1j}(\theta_0) \cos\theta_0 \, d(\cos\theta_0)$ the integrated transmission probability $\bar{w}_{1j}$. Two factors thus determine the heat flux of each mode, namely, the rate phonons reach the surface $(\pi^2 k_b^4 T_1^4 / 120\hbar^3 c_{1j}^2)$ and $\bar{w}_{1j}$. A similar expression can be derived for the energy flux from material 2 to material 1. When the temperature is the same on both sides of the interface there can be no net heat flux so that $\dot{Q}_{1\to 2} = \dot{Q}_{2\to 1}$. This implies

$$\sum_j (\bar{w}_{1j}/c_{1j}^2) = \sum_f (\bar{w}_{2f}/c_{2f}^2) \tag{4}$$

The material with the lower sound velocity has the smaller *integrated* transmission probability. This results from the total reflection of phonons incident from that material at angles greater than a critical angle θ_c.

When the temperatures in the two materials are unequal the net heat flux $\dot{Q}$ across an interface of area A is given by

$$\dot{Q} = (\pi^2 k_b^4 A/120\hbar^3) \sum_j (\bar{w}_{1j}/c_{1j}^2)(T_1^4 - T_2^4) \tag{5}$$

If the difference in temperature ΔT is much smaller than the average temperature T, then

$$\dot{Q} = (\pi^2 k_b^4 A/30\hbar^3) \sum_j (\bar{w}_{1j}/c_{1j}^2) T^3 \Delta T \tag{6}$$

The thermal boundary resistance is, therefore,

$$R_B \equiv A\Delta T/\dot{Q} = (30\hbar^3/\pi^2 k_b^4) T^{-3} \left(\sum_j \bar{w}_{1j}/c_{1j}^2 \right)^{-1} \tag{7}$$

If the transmission probability $\bar{w}_{1j}$ is independent of the temperature the resistance increases rapidly, $R_B \propto T^{-3}$, as the temperature is lowered.

We use the classical theory of acoustic waves to obtain the scattering probability of phonons, that is, to calculate $\bar{w}_{1j}$. An acoustic wave incident on the interface may generate as many as four outgoing waves, as shown in Fig. 1. The waves are assumed to have displacement u at position $\mathbf{r}$ and time t of the form

$$u = B\, e^{i\mathbf{k}\cdot\mathbf{r} - i\omega t - (\alpha\hat{k}\cdot\mathbf{r}/2)} \tag{8}$$

where $\hat{k}$ is a unit vector in the direction of $\mathbf{k}$. The constant α is the energy attenuation per unit distance; α, in general, will be different for transverse and longitudinal modes. The attenuated displacements can alternatively be expressed in terms of complex sound velocities,* that is,

$$u = B\, e^{i(\omega\hat{k}\cdot\mathbf{r}/c') - i\omega t} \tag{9}$$

where

$$c' = c[1 + (i\alpha c/2\omega)]^{-1} = c[1 + (i\lambda/4\pi l)]^{-1} \tag{10}$$

The phonon wavelength is λ, and l is the mean free path for attenuation of energy. Note that it is the ratio λ/l which is of importance. The replacement of c by c' is the basic difference between the present theory and previous calculations of R_B. In an anisotropic solid, c' would in general depend on the direction of propagation. However, for the polycrystalline materials to be discussed below we approximate the situation by using an isotropic model.

Four boundary conditions are applied for each incident mode, namely, that the displacements and stresses both parallel and perpendicular to the

*The use of a complex velocity in computing R_B has previously been suggested,[13,14] but not carried out.

interface should be identical on both sides of the boundary. The resulting equations consume too much space to be included here and, besides, are available elsewhere.[15,16] Relations between the many angles of Fig. 1 are obtained by requiring the phase of each of the waves to have the same repetition rate along the x axis. This gives an acoustic Snell's law for each incident mode:

$$\begin{aligned}(\sin\theta_0/c_0') &= (\sin\theta_{1l}/c_{1l}') = (\sin\theta_{1t}/c_{1t}') \\ &= (\sin\theta_{2l}/c_{2l}') = (\sin\theta_{2t}/c_{2t}')\end{aligned} \tag{11}$$

In general, these angles are complex and, for an attenuating media, do not correspond to the directions of propagation of the acoustic energy.

Finding $\bar{w}$ thus involves solving, with the use of a computer,[15] four complex equations in four complex unknowns for each of the three possible incident modes and integrating the results over all angles of incidence. Many mathematical difficulties are avoided by not analyzing the energy flow in an attenuating medium directly, that is, we assume that the wave is incident on the interface from a material with *zero* phonon attenuation. The transmission probability will then be calculated from the amplitudes of only the *reflected* waves using

$$w(\theta_0) = 1 - [|S_{1l}(\theta_{1l})|^2/|S_0(\theta_0)|^2] - [|S_{1t}(\theta_{1t})|^2/|S_0(\theta_0)^2] \tag{12}$$

where the energy flux S_{ij} normal to the interface is given by

$$S_{ij} = (\omega^2\rho_i c_{ij}/2)|B_{ij}|^2 \operatorname{Re}(\cos\theta_{ij}) \tag{13}$$

B_{ij} is the wave amplitude and ρ_i is the mass density of material i. As will be shown shortly, no information concerning R_B is lost by this maneuver since the transmission is independent of the attenuation in the material having the lower sound velocity.

The transmission probability for the relatively simple case of a wave incident from a liquid on a liquid–solid interface can be written explicitly as

$$w(\theta_0) = 4\operatorname{Re}(\beta)(|1+\beta|)^{-2} \tag{14}$$

where

$$\begin{aligned}\beta = (\rho_2/\rho_1)(\cos\theta_0/c_0)\{&c_l'[1 - 2(c_t'\sin\theta_0/c_0)^2]^2 \\ &\times [1 - (c_l'\sin\theta_0/c_0)^2]^{-1/2} + 4c_t'[(c_t'\sin\theta_0/c_0)^2 \\ &- (c_t'\sin\theta_0/c_0)^4][1 - (c_t'\sin\theta_0/c_0)^2]^{-1/2}\}\end{aligned} \tag{15}$$

The subscripts l and t refer to longitudinal and transverse sound velocities in the solid, and c_0 is the velocity of the longitudinal mode in the liquid.*

*This expression for the transmission probability results when the transverse velocity in the liquid is set equal to zero in the general solid–solid computer program.[15,17]

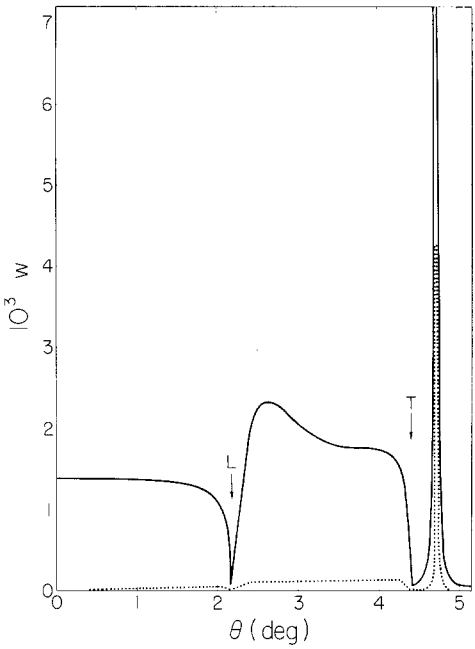

Fig. 2. The solid curve indicates the ratio w of energy absorbed by copper to the energy incident at angle θ from liquid ^{3}He at 0 atm with weak phonon attenuation in the copper. The Rayleigh peak, shown truncated on the plot, rises to $10^3 w = 600$. The broken line results from multiplying the solid curve by $\sin\theta \cos\theta$, which is indicative of the relative contribution at various angles to the total heat flux. In this case the peak rises to $10^3 w = 50$.

Equation (14) is plotted for a liquid ^{3}He–Cu interface as a function of angle in Fig. 2, where we have used a small attenuation for both phonon modes in the solid, namely, $\lambda/l = 5 \times 10^{-3}$. The curve for angles less than 4.4° is the same as it would be with zero attenuation. The acoustic mismatch theory with $\alpha = 0$, however, gives $w = 0$ for angles larger than 4.4°. The critical angles beyond which propagating longitudinal L and transverse T waves cannot be excited in the solid are indicated in Fig. 2. Briefly, such phonons are not transmitted because the conditions of conservation of momentum and energy cannot be simultaneously satisfied at the boundary.

The peak near 4.7° appears only when attenuation is included. This peak is caused by the resonant excitation of interface waves by phonons incident from the liquid ^{3}He. These waves were discussed in general by Stoneley.[18]

But since the density of liquid ^{3}He is small relative to that of copper, the interface wave may quite accurately be considered to be a Rayleigh wave on the surface of copper situated in vacuum. The peak in Fig. 2 occurs when the projection, parallel to the surface of the solid, of the wave vector in the liquid is equal to the wave vector for the Rayleigh wave.

It is perhaps not obvious that the curve of Fig. 2 properly describes the actual energy transmission, especially near the Rayleigh peak. However, using *measured* values of bulk attenuation Becker and Richardson have found excellent agreement between the curve predicted by this theory and that observed for reflection of ultrasonic waves at water–metal interfaces.[19] Furthermore, phase shifts predicted by the theory are rather unusual but have been verified in detail experimentally.[20] Thus the present theory is correct in the low-temperature or long-wavelength limit.

To calculate R_B one must next integrate $w(\theta_0)$ over solid angle. The relative contribution to the heat flux at each angle of incidence is found by multiplying $w(\theta_0)$ by $\sin\theta_0 \cos\theta_0$ [see Eq. (2)], which has been done in Fig. 2 (dashed curve). This was done to emphasize why R_B is so large for liquid He. There is not only a factor of $\approx 10^3$ reduction in thermal transport due to acoustic mismatch, but also a reduction because of the small solid angle included within the critical angle θ_c. The Rayleigh wave makes an important contribution to R_B^{-1}, in the presence of attenuation, not only because $w \approx 1$ but also because $\sin\theta_0$ is finite.

The angular integration of Fig. 2 has been performed numerically using a computer.[15] The resultant averaged transmission probability $\bar{w}$ for helium–copper interfaces is plotted as a function of λ/l in Fig. 3. Since it is apparent from the figure that $\bar{w}$ can vary considerably, in general we should also have included $\bar{w}$ in the integration over phonon frequency [Eq. (2)] in order to find R_B. However, if λ/l is either independent of frequency or does not change rapidly near the maximum in the phonon distribution, the present technique does not introduce a significant error. With the assumption of a slowly varying $\bar{w}$, the expected values of R_BT^3 for helium–copper interfaces can be found on the scale on the left-hand side of Fig. 3.

Curves *A*, *B*, and *C* of Fig. 3 were computed for a low-pressure liquid ^{3}He–Cu interface. Curve *A* was calculated assuming attenuation resides *only* in the liquid He. This attenuation has little effect on R_B. In fact, R_B is the value obtained by Khalatnikov[21] for the case of zero attenuation. This is because all phonons incident on the interface from the material with the higher sound velocity may be refracted into the other material without creating surface waves or disturbances. Thus, as was mentioned above, we may largely ignore any attenuation in the material having the *smaller* acoustic velocity. The remaining curves in Fig. 3 were calculated assuming attenuation existed only in the copper.

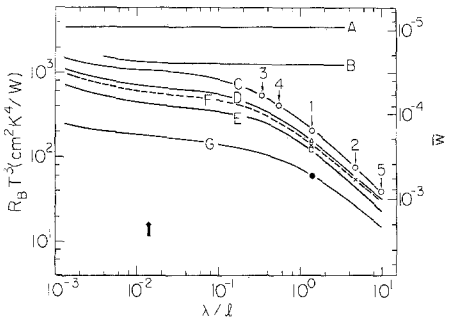

Fig. 3. Computed curves of $R_B T^3$ or $\bar{w}$, with quantum-mechanical corrections, as a function of phonon wavelength λ divided by phonon mean free path l for a copper interface with five different states of helium. λ/l was taken to be the same for both the transverse and longitudinal modes. Curve *C*, liquid ^{3}He at 0 atm; curve *D*, liquid ^{3}He at 6.5 atm; curve *E*, liquid ^{3}He at 27 atm; curve *F*, liquid ^{4}He at 0 atm; curve *G*, solid ^{3}He. Shown at 1 are the low-temperature data of Anderson *et al.*[22]: (○) liquid ^{3}He at 0 atm; (△) liquid ^{3}He at 6.5 atm; (□) liquid ^{3}He at 27 atm; (×) liquid ^{4}He at 0 atm; (●) solid ^{3}He. At 2 are the data of Wheatley, *et al.*,[23] the symbols having essentially the same meaning as for 1. Other symbols and curves are discussed in the text.

In calculating curve *B* of Fig. 3 the integration over angle was carried out only from 0 to 7° rather than from 0 to 90° and thus includes just the phonons refracted into the solid (i.e., for incident angles $\theta_0 \leq 4.4°$) plus the contribution due to the excitation of Rayleigh waves (see Fig. 2). At large phonon attenuation the magnitude of the integration saturates at a constant value, as shown by curve *B*. This value is just that calculated by Khalatnikov[21] when he included the Rayleigh wave contribution in the limit of very large attenuation.* Our theory thus contains the two limits found by Khalatnikov, namely, that for zero attenuation (*A* in Fig. 3) and that including the contribution by Rayleigh waves for very large attenuation (*B* in Fig. 3).

The remaining curves on Fig. 3 have been computed by integrating over all angles of incidence. The difference between curves *B* and *C* thus comes about from the integration over incident angles in the range 7–90°. These phonons cause a nonpropagating disturbance in the second material which

*Khalatnikov used a contour of integration which encompassed the pole associated with the Rayleigh wave.

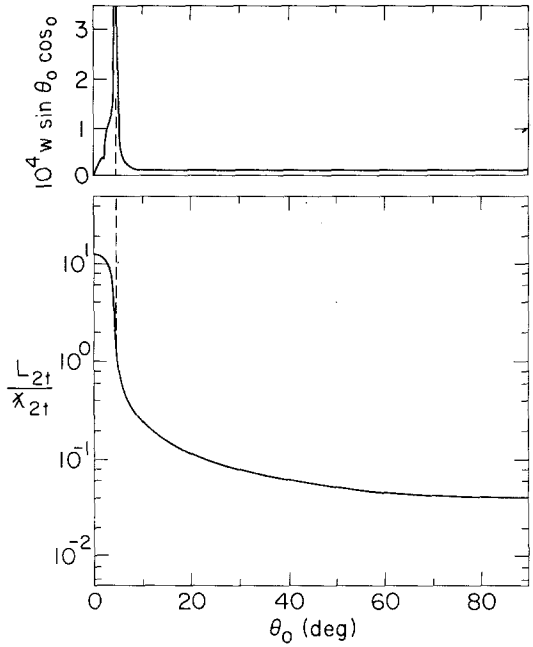

Fig. 4. Transmitted heat flux (upper curve) and penetration depth (lower curve) for a transverse wave at a ^{3}He–Cu interface as a function of angle of incidence θ_0. The length L_{2t} is defined as the depth at which the *energy* decreases by e^{-1}, and has been normalized to λ, the transverse wavelength divided by 2π. The vertical dashed line is a visual aid showing that the penetration depth at the angle of the Rayleigh peak is $\approx \lambda_{2t}$.

decreases exponentially perpendicular to the interface. When attenuation is present, substantial energy can be absorbed from this surface disturbance into the second material. At the top of Fig. 4 this additional heat transmission is shown as a function of incident angle for the arbitrary choice $\lambda/l = 0.5$.

The surface waves and disturbances do not propagate very deeply into the solid. This is demonstrated at the bottom of Fig. 4 for the transverse wave in the solid. The penetration depth at the smallest angles is determined largely by the value of phonon attenuation, in this case $\lambda/l = 0.5$. The penetration depth at large angles is nearly independent of attenuation and is determined mainly by the sound velocity in the solid, c_t. A similar curve can be drawn for the longitudinal disturbance, which penetrates to about the same depth at large angles. The lower plot gives no information about the *amplitude* of the transverse disturbance, which goes to zero at $\theta_0 = 0$. Also, the function $w(\theta_0) \sin\theta_0 \cos\theta_0$ does drop to zero at $\theta_0 = 90°$.

The penetration depth for the Rayleigh wave is thus of order of the wavelength of a transverse wave in the solid. At 0.1 K this is ≈ 1000 Å. At the same temperature and larger angles the nonpropagating disturbances which contribute substantially to R_B^{-1} penetrate only ≈ 50 Å. This effect has two important but related consequences. First, it is the attenuation *very near* the interface which is important in R_B. Second, although we have assumed a homogeneous attenuation in our derivation, in fact the attenuation need be approximately uniform only for a depth of $\approx \lambda$ for the theory to be valid.

Since the attenuation of transverse and longitudinal phonons may be different, a plot such as that of Fig. 3 actually depicts a cut through a surface having $R_B T^3$ as the vertical axis and λ_t/l_t and λ_l/l_l as the two horizontal axes. Three such cuts are shown in Fig. 5 for three ratios of $(\lambda_t/l_t)/(\lambda_l/l_l)$. The major effect of changing this ratio is to shift the curve horizontally. Thus little information is lost in presenting a single curve of $R_B T^3$ vs. λ_l/l_l, provided the ratio of longitudinal to transverse attenuation is also given.

The results of computations for He–Cu boundaries are shown in Fig. 3 for liquid ^{4}He near zero pressure, liquid ^{3}He at three different pressures (and hence different ρ and c), and, although it is somewhat out of place at this point in the text, solid ^{3}He. Also shown on Fig. 3 are the only available data with which the theory may be compared.[22,23] The theory should be valid in the limit of low temperatures, so only low-temperatures ($T \lesssim 0.1$ K) values of experimental R_B are used. The uncertainty in these values is larger than the size of the symbols used in Fig. 3, this size having been chosen for reasons of clarity.

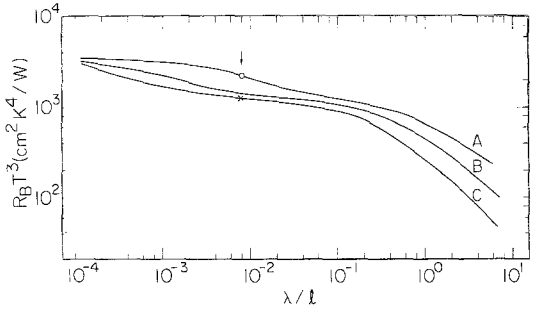

Fig. 5. Kapitza resistance R_B multiplied by T^3 for a liquid ^{3}He–Cu interface (at 0 atm) as a function of *longitudinal* phonon wavelength λ divided by longitudinal phonon mean free path l for three ratios of transverse λ/l to longitudinal λ/l. Curve A, $(\lambda_t/l_t)/(\lambda_l/l_l) = 0$; curve B, $(\lambda_t/l_t)/(\lambda_l/l_l) = 0.5$; curve C, $(\lambda_t/l_t)/(\lambda_l/l_l) = 1.5$. The theoretical value of λ/l for attenuation of longitudinal ultrasonic waves by electrons is indicated by the arrow.

One does not know the values of λ/l appropriate to the copper surfaces used to obtain the experimental points shown in Fig. 3. However, one may use, say, the value of R_B for liquid ^{4}He to determine λ/l. Having thus selected a value for the only unknown parameter, the ^{3}He data fall as indicated in Fig. 3. Note that the *solid* ^{3}He point is in good agreement with theory.

The *liquid* ^{3}He data, on the other hand, would lie $\approx 30\%$ below the calculated values unless quantum-mechanical corrections were made to allow for the fact that ^{3}He is a Fermi liquid. Still, this agreement is considerably better than the $\approx 1000\%$ disagreement between the data and the usual acoustic mismatch theory with no phonon attenuation present.

We have attempted to account for the quantum-mechanical properties of liquid ^{3}He by applying corrections directly to the final results of the attenuated phonon theory. For example, theory gives an additional heat flux due to quasiparticles of $\approx 15\%$ at 0 psi,[24,25] and so curve C of Fig. 3 has been corrected by this amount for all values of λ/l (i.e., it is assumed that the quasiparticles couple to phonons in the solid). This correction is $\approx 5\%$ at 6.5 atm and $\approx 0\%$ at 27 atm. Fomin[26] has calculated the effect due to the transverse zero-sound mode in ^{3}He and has expressed the correction in terms of the effectiveness of normal or ordinary transverse modes. To apply the correction we first calculated the additional heat flow due to transverse modes in the liquid. This extra heat flow was then reduced by the effectiveness factor α from Fomin's theory before adding it to the heat flow from the usual longitudinal mode and the quasiparticles. This correction varied with λ/l and was greatest for the 27 atm ^{3}He where the correction to R_BT^3 was 24% at $\lambda/l = 1.5$. The curves of Fig. 3 for liquid ^{3}He reflect the quasiparticle and transverse zero-sound corrections. The agreement between theory and experiment is excellent, including the pressure dependence. Although this agreement is somewhat fortuitous in light of the uncertainties in the experimental values, it perhaps does represent the first experimental evidence for the presence of transverse zero sound in liquid ^{3}He.

The data of Wheatley *et al.*[23] (2 on Fig. 3) were obtained for a machined surface, while the data of Anderson *et al.*[22] (1 on Fig. 3) were obtained on an electropolished surface. Hence it may be reasonable that the data at 2 should lie at larger attenuation (λ/l) and lower R_BT^3. Several other low-temperature experimental measurements[10] have been placed on the curve, indicating the large spread in λ/l necessary to account for some of the observed values of R_BT^3. Point 3 was obtained on an annealed, electropolished surface, 4 for the same surface gently cleaned with a tissue, and 5 for the same surface "sandblasted" with 47-μm waterborne abrasive.* Annealing again reversed

*J. D. Siegwarth and R. Radebaugh[27] have observed a similar dependence of R_B on the degree of strain hardening in Cu caused by the precipitation of Cr.

this trend and reestablished a large value of $R_B T^3$. Although these last data points in no way test the present theory, they do demonstrate the range of λ/l required to fit the data and emphasize that increased damage near the surface (and presumably increased phonon attenuation) in fact decreases R_B remarkably.

An important aspect of the present approach is its independence of the details of any particular attenuating mechanism. It should be emphasized that if attenuation is important in R_B for a particular interface, $R_B \propto T^{-3}$ only if $l \propto \lambda$, i.e., only if the phonon attenuation is proportional to frequency [see Eq. (10)]. This can be the case for either electron or dislocation scattering of phonons. In general, however, one should not expect $R_B \propto T^{-3}$ in situations where phonon attenuation makes an appreciable contribution to R_B^{-1}. Indeed, most experiments involving He do not give a convincing T^{-3} power law for R_B even at low temperatures.

A phonon attenuation mechanism common to all metals is that due to electrons. Pippard[28] has developed a theory for attenuation of acoustic waves by electrons. The general qualitative dependencies predicted by the theory have been well verified in direct acoustic attenuation studies for frequencies up to 10^9 Hz[29] and for thermal phonons in experiments on lattice conductivity of alloys above ≈ 1 K.[30] However, in the temperature range of interest in this paper, 0.01–0.2 K, the attenuation has not been measured. Therefore the curves plotted in Fig. 6 were calculated from Pippard's equations for the case of copper in the free-electron limit. The thermal

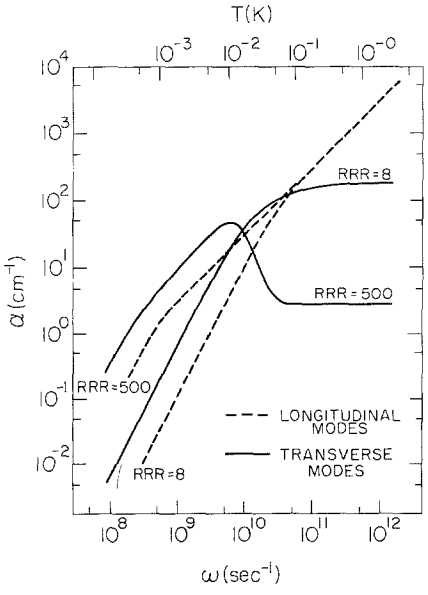

Fig. 6. Attenuation α of transverse and longitudinal acoustic phonons in copper as a function of angular frequency ω or temperature T. The curves are based on Pippard's free-electron theory. The residual resistivity ratio *RRR* is defined as the ratio of electrical resistivity at 300 K to that at 4 K.

phonons important in heat conduction have a dominant frequency of $\omega \approx 4kT/\hbar \approx 5 \times 10^{11} T (\text{sec}^{-1})$, so an approximate temperature scale is shown at the top of the figure.

Generalization of Pippard's theory to non-free-electron metals depends on the deformation parameter and the actual shape of the Fermi surface, and the corrections can be very important in some metals. Tungsten and molybdenum, for example, have a measured ultrasonic attenuation about 100 times the free-electron prediction.[31] The fall-off of transverse attenuation at large ω is expected to be weaker when corrections to the free-electron model are included.[32] Although the corrections for copper are small, Fig. 6 is intended nevertheless as a qualitative rather than quantitative display. It should also be remembered that most metals used in a measurement of R_B are polycrystalline.

The value of the transverse phonon attenuation is quite important in determining the attenuation contribution to R_B^{-1}. For example, the magnitude of transverse attenuation was the decisive consideration in the calculations by Little[14] and Andreev[33] of the Rayleigh surface-wave contribution to R_B^{-1}, because this surface wave is primarily transverse in character. In those computations, which have been reviewed by Challis and Cheeke,[34] electrons were the only phonon damping mechanism considered. Little assumed there was no attenuation of transverse phonons. The result of this assumption can be seen on Fig. 5, where longitudinal attenuation by electrons only (from Fig. 6) is represented by the arrow. Zero transverse attenuation is represented by (0) on curve A; at the position of the arrow, $R_B T^3$ has been reduced 30%. This is in rough agreement with Little's result. On the other hand, a large transverse attenuation corresponds to (x) on curve C of Fig. 5. The decrease in R_B at the position of the arrow agrees with Andreev's result for strong electron–phonon coupling. Andreev, however, included only the additional contribution of the Rayleigh wave and thus could not obtain a value of $R_B T^3$ smaller than that obtained by Khalatnikov,[21] who assumed complete attenuation of the Rayleigh wave (the limiting value of curve B in Fig. 3).

The value of λ/l due to electronic attenuation is shown by the large arrow in Fig. 3. It will be noted that the value of λ/l required to fit $R_B T^3$ obtained using the best copper surface prepared to date (point 3) is about a factor of 10 larger than λ/l due to electrons. On the other hand, $R_B T^3$ for this particular surface is only a factor of two smaller than calculated assuming *only* electronic attenuation were present.

The question remains whether it is possible to have an effective $\lambda/l \approx 1$ near the interface as required by points 1, 2, or 5 of Fig. 3. This requires an answer based on experiment, and two pertinent measurements have been carried out. Both Wigmore[35] and Anderson and Smith[36] present evidence

that when phonons are incident on a "sandblasted" surface from within a specimen (situated in vacuum), the phonons are at least partially thermalized. The abraded surface appears black in the optical sense. This is simply another way of saying that the phonon attenuation is extremely large near a damaged surface. Even at ultrasonic frequencies much lower than the thermal frequencies appropriate to R_B the reflectivity has been found to be highly sensitive to surface damage.[37]

It is likely that dislocations play an important role in R_B of a physically damaged surface. Haug and Weiss[38] have independently made a computation of R_B which, though basically identical to our approach, considers the contribution to R_B^{-1} due to the attenuation of phonons by dislocations alone. This requires a model of the phonon-dislocation interaction in metals at thermal frequencies, and a proven model is not available at present. Nevertheless, the qualitative features of $R_B T^3$ vs. attenuation for the two computations are in complete agreement.

In a metal the dislocation motion is strongly damped by electrons. Hence any energy transfer due to the excitation of dislocations in the metal surface by phonons incident from the helium would be rapidly dumped into the electron gas. It is interesting to note that such a parallel mechanism could conceivably lead to heat flows in excess of the blackbody or phonon radiation limit [$\bar{w} = 1$ in Eq. (7)], although this has never been observed. Also the contribution of dislocation attenuation to R_B^{-1} would likely change in magnitude upon transition of the metal into the superconducting state. Thus although the contribution to R_B^{-1} from electron attenuation would tend to zero, the dislocation contribution could become either larger or smaller and exhibit a strong temperature dependence.[39]

In the foregoing we have directed our attention to phonons incident from the liquid on the interface, there to interact with an electron or dislocation. The reverse process also occurs. An electron incident on the interface sees a greater density of phonon states than in the bulk. Some of these states are represented by phonons propagating freely in the He in a direction away from the interface, but having a nonpropagating, exponentially decreasing tail within the metal. The same is true of a local phonon mode associated with a dislocation. Near the surface this mode has a greater number of phonon states into which to decay. To describe this reverse process quantitatively would require exact microscopic knowledge of the attenuation mechanism. The process actually causing the apparent large attenuation very near the interface may be difficult to characterize for a particular metal surface.

The present theory has given a reasonable explanation to several aspects of the He–solid R_B. This theory, however, has been compared with experiment only below ≈ 0.1 K. Above 0.1 K the experimentally measured $R_B T^3$ decreases by a factor of ≈ 10 and again becomes nearly constant above 1 K.[10,22] At 1 K the surface disturbances which contribute significantly

to R_B^{-1} penetrate into the solid only a couple of atomic layers. One hesitates to extend the theory into this temperature regime. In addition, other mechanisms[10] may contribute to R_B^{-1} above 0.1 K, which makes the value of any comparison with the present theory at high temperatures even more dubious.

There is one additional calculation of R_B for a He–solid interface which we have not mentioned, namely, the original calculation by Khalatnikov[40] in which the solid surface was treated as a (thermally) vibrating piston which pumped acoustic energy into the liquid He. The motion of the piston was calculated assuming complete reflection of all phonons incident on the surface from the solid. This computational technique agreed with that of the later more exact acoustic mismatch theory[21] only because of the very large difference in acoustic impedances between liquid He and a solid. Hence we see from the later calculation that the energy does in fact enter the He nearly perpendicular to the interface (see Fig. 2). However, the technique of the piston fails whenever the assumption of complete reflection of phonons from the surface is no longer valid (as in the case of He–solid and large phonon attenuation) or when phonons are excited having wave vectors not directed perpendicular to the interface (as in the presence of attenuation). Although this earlier computation is invitingly simple conceptually, it is of little use in obtaining quantitative values of R_B for He–solid boundaries.

The remainder of this section will consider the application of the attenuated phonon theory to solid–solid interfaces, and, in particular, to those interfaces investigated experimentally and discussed in the next section. The acoustic mismatch theory without attenuation has been applied to solid–solid interfaces by Little[1] and, in more detail, by Weis.[41]

The application of the present theory to several combinations of metals in contact with a particular dielectric are shown by the curves in Fig. 7. These

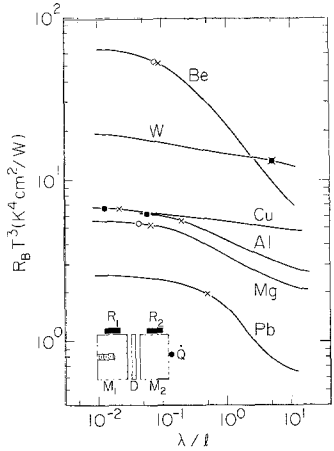

Fig. 7. Computed curves of R_B multiplied by T^3 vs. the ratio λ/l. The value of λ/l for each metal is indicated by (●) if extrapolated from measured data, or by (○) if estimated from the free-electron theory. The present experimental values of $R_B T^3$ for each metal are indicated by (×) and were obtained using the arrangement shown schematically by the insert. M_1 and M_2, metal blocks; M_1 was attached to a dilution refrigerator. R_1 and R_2, resistance thermometers; $\dot{Q}$, electrical heater; D, dielectric layer.

correspond to the materials used in the measurements described in Section 3. Also shown by circles in Fig. 7 are the attenuations λ/l arising from the electron–phonon interaction in these metals. The vertical position of the circles thus indicates the theoretically predicted value of $R_B T^3$ for each metal provided that electrons are the major cause of phonon attenuation. Since the values of λ/l are not known for the frequency range of interest, they have been estimated either from ultrasonic measurements or from the free-electron theory. The longitudinal and transverse attenuation were assumed to vary inversely with frequency and to have the same magnitude which could be either an overestimate or underestimate depending on the appearance of Fig. 6 when applied to the metal in question. The values and sources of the information used in estimating the phonon attenuations are given in the appendix.

Although in Fig. 7 an increase in λ/l decreases $R_B T^3$ for the Be interface in an amount similar to that for liquid ^{3}He, the Cu interface is little affected by attenuation. The reason for this may be seen in Fig. 8. The additional contribution due to the Stoneley wave of the copper–dielectric boundary is only a small fraction, 2%, of the total thermal transfer across the interface as compared to 67% for a ^{3}He–Cu interface with the same value of attenuation. Hence attenuating mechanisms very close to the surface are of less importance for the dielectric–copper interface. Also, $R_B T^3$ should be independent

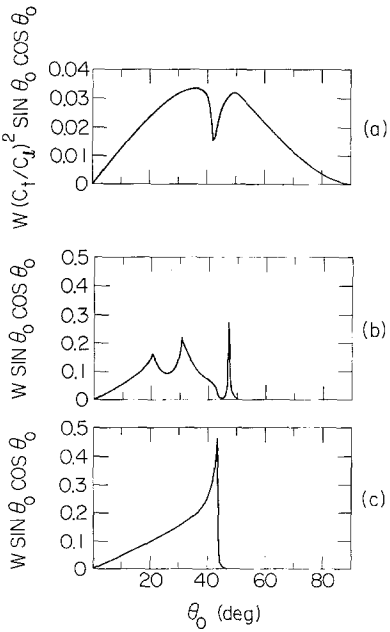

Fig. 8. Thermal flux transmitted across a Cu–epoxy interface vs. the incident angle θ_0. The ratio λ/l was taken as 10^{-2}. (*a*) Incident longitudinal phonons; (*b*), (*c*) incident transverse phonons. The vertical scale of curve (*a*) is expanded; the incident longitudinal phonons contribute only 13% to the total heat flux. The contribution due to Stoneley surface waves is represented by the peak near 47° in curve (*b*).

of temperature for a Cu–solid junction, whereas for He–Cu, for example, the temperature dependence of $R_B T^3$ depends more critically on the frequency dependence of l.

The additional transfer of heat across a solid–solid interface in the presence of electrons has been calculated by Park and Narahara.[17] They used the technique of Little and included only the interaction of electrons with longitudinal phonons.

Difficulties may arise when applying even the usual acoustic mismatch theory. For example, the acoustic mismatch theory will hold only as long as the temperatures T_1 and T_2 adequately characterize the phonons *incident* on the interface. Such is the case for the half of the junction which may be a metal. Because of the strong inelastic scattering of phonons by the electrons, the phonons incident on the boundary from the metal will have the temperature of the electrons. A similar comment applies to the case of liquid ^{3}He. In other cases the source of the phonons incident on the interface must be considered in ascribing magnitudes to T_1 and T_2. It may then be misleading to think in terms of a temperature profile near the interface if the phonons are not in thermal equilibrium. This is analogous to a thermal conductivity measurement in which phonon scattering occurs only at the surfaces of the specimen. For $\Delta T/T$ small this problem is less important since the phonon population deviates only slightly from a thermal equilibrium distribution. However, the temperature to be ascribed to this distribution will remain ambiguous unless the phonon scattering in the bulk is highly inelastic (as in metals) and/or R_B is large [$w(0)$ small] so that most incident phonons are reflected by the boundary. It should be emphasized that we are not referring here to an accidental decrease in phonon mean free path near an interface which introduces errors if one attempts to extrapolate an experimentally determined temperature gradient to that interface and which has apparently occurred in measurements involving superconductors.[12]

The above considerations dictated the metal–dielectric–metal sandwich configuration used in the measurements and shown by the insert in Fig. 7. For such a sandwich one obtains Eq. (7) with $\bar{w} = 1$ if the phonon mean free path in the dielectric is much larger than the thickness of this layer and if the dielectric has the same acoustical properties as the metal. If, however, the acoustic properties differ, phonons incident on the first interface will have a probability $\bar{w}$ of entering the dielectric. Since these phonons propagate within a cone of half-angle θ_c, they also have a probability $\bar{w}$ of refracting into the metal at the second surface and a probability $1 - \bar{w}$ of being reflected back into the dielectric. This process may be repeated for many reflections giving an effective transmission probability[42] $\bar{w}' = \bar{w}(2 - \bar{w})^{-1}$. The total thermal impedance across the sandwich becomes

$$A\Delta T/\dot{Q} = (2 - \bar{w})R_B \tag{16}$$

where R_B is computed for a single interface. Both $\bar{w}$ and R_B are obtained from the attenuated phonon model. One example of a measurement of R_B involving a dielectric layer having a long phonon mean free path is the experiment of Anderson *et al.* on liquid ^{4}He.[22] In that case $\bar{w}$ was very small (Fig. 3) and $A\Delta T/\dot{Q} = 2R_B$.

If the mean free path in the dielectric layer is not large, the phonons within the dielectric approach a temperature intermediate between T_1 and T_2 and $A\Delta T/\dot{Q}$ should increase and approach the value $2R_B$ as the mean free path becomes shorter. However, the bulk thermal impedance now becomes important so that in the limit of a mean free path short compared to the thickness L,

$$A\Delta T/\dot{Q} = 2R_B + LK^{-1} \tag{17}$$

where K is the thermal conductivity of the dielectric. We have assumed here either that $2(T_1 - T_2)(T_1 + T_2)^{-1}$ is small or that the scattering in the dielectric is inelastic. Equations (16) and (17) will be applied to an analysis of the experimental solid–solid boundary resistance data in Section 3.

3. EXPERIMENT

The experimental arrangement for studying R_B of solid–solid boundaries is shown schematically in Fig. 7. The sandwich arrangement consists of two metal blocks of the same metal but isolated electrically with a thin Mylar sheet. Epoxy adhesive (Epibond 121) bonded the surfaces together. The surface of each block was polished mechanically to optical flatness ($< 10^{-4}$ cm). Most blocks were then annealed in vacuum, although some had other surface treatments as discussed below. The Mylar sheet was first epoxied to one block and the epoxy allowed to cure under slight mechanical pressure. If optical inspection then indicated no air pockets or other flaws, the second block was epoxied in place under slight mechanical pressure. The resulting epoxy bonds were less than 10^{-4} cm thick. Bonds could be broken without damage to the metal surface by the patient application of solvent.

Temperatures were measured using modified carbon resistance thermometers[43] calibrated against a single-crystal sphere of cerium magnesium nitrate in a magnetic thermometer.[44] Only the thermometer on the block at the right of Fig. 7 was calibrated; the left thermometer only served to keep the left block at a constant temperature, while obtaining a datum, by electronically regulating heater power to the dilution refrigerator. In calculating ΔT only the change ΔR in the resistance R of the thermometer was used, along with the smoothed derivative $d(\ln R)/(\ln T)$ of the calibration curve.[45]

The thermal conductivities of the metal specimens were measured so as to be certain that the metal blocks would be effectively isothermal. Also

it was determined that, within the $\approx 5\%$ reproducibility of the measurements from sample to sample, the R_B of the Mylar–epoxy surfaces could be neglected. This was shown by covering only part of the surface with Mylar spacers, or by comparing measurements involving two sheets of Mylar (i.e., four Mylar–epoxy boundaries) with a measurement using a single sheet having the same total thickness as the two layers.

Except as noted explicitly below, all measurements were made on normal metals. The Al and Pb samples were therefore placed in a magnetic field of up to 2000 G. Under these conditions the temperature calibration was maintained using a carbon resistance thermometer glued to the end of heavy copper wire and positioned outside the region of magnetic field. The samples were maintained in a high vacuum produced by pumping the thermal exchange gas at a temperature of ≈ 20 K, and were located within a closed thermal shield maintained at a temperature of 0.7 K.[46] Most data were obtained between 0.05 and 0.2 K. At lower temperatures the thermal relaxation time of the sandwich became rather long, and at higher temperatures the $\dot{Q}$ required to provide a convenient ΔT became greater than the available refrigeration capacity. $\Delta T/T$ was varied between 5 and 10% at all temperatures, but no $\dot{Q}$ dependence was observed in the ratio $\Delta T/\dot{Q}$.[47]

We first discuss three epoxy–Mg interfaces since R_B is small for this boundary, and hence any confusion associated with the dielectric layer should be emphasized in the data. From Eq. (17) and the knowledge that, roughly, $K \propto T^2$, for Mylar and epoxy we can expect

$$A\Delta T/\dot{Q} = aT^{-3} + bT^{-2} \tag{18}$$

where $A\Delta T/\dot{Q}$ is obtained from experiment. A plot of $AT^3\Delta T/\dot{Q}$ vs. T is shown in Fig. 9 for the same Mg samples and three different thicknesses of Mylar. The intercept is the same in each case and will be designated a_{exp}. In other words, $\lim_{T\to 0}(AT^3\Delta T/\dot{Q}) \equiv a_{\text{exp}}$. Since we expect the T^2 dependence of K to result from a phonon mean free path inversely proportional to frequency, Eq. (16) should be appropriate in the low-temperature limit. For convenience we define $(2 - \bar{w})R_BT^3 \equiv a_{\text{th}}$, the theoretical or predicted low-temperature limit.

From Eq. (17) we expect the slope of the three lines in Fig. 9 to be proportional to the thickness L of the Mylar. This is exhibited at the bottom of Fig. 9. But instead of $b = \beta L$, one sees $b = \beta_0 + \beta L$. Indeed, $\beta = T^2K^{-1}$, where K is the measured thermal conductivity of Mylar.[48] The origin of the constant β_0, on the other hand, cannot be established. The presence of β_0 indicates a slight increase in $AT^3\Delta T/\dot{Q}$ with increasing T even for a vanishingly thin layer of dielectric. It may be that R_B does not in fact vary exactly as T^{-3}. However, the calculations represented by Fig. 7 indicate that the Mg–epoxy interface should not be very sensitive to phonon attenuation and hence to

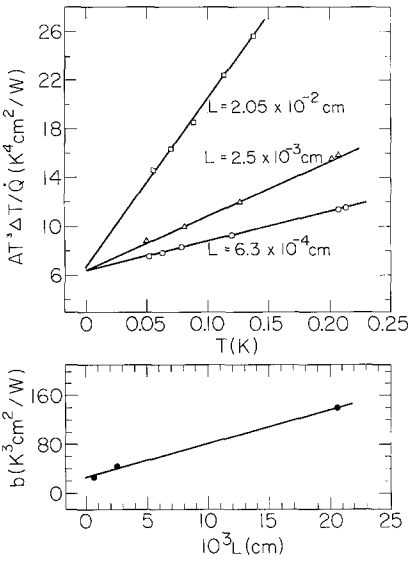

Fig. 9. Top, ratio of the experimental values $AT^3\Delta T/\dot{Q}$ vs. temperature T for three different thicknesses of Mylar in a Mg sandwich. Bottom, slope b of the above three lines vs. the Mylar thickness L. Note that the zero on each scale has been offset to improve clarity.

the temperature dependence of λ/l. Rather, it may be that the presence of β_0 reflects the change from Eq. (16) to Eq. (17) as the mean free path of phonons in the dielectric decreases with increasing temperature. We refer here to the physical phenomenon related to the change from $(2 - \bar{w})R_B$ to $2R_B$ and *not* that related to the term LK^{-1}. However, extrapolating the data of Fig. 9 to $T = 0$ allows us to ignore both of these effects, and hence it is a_{exp} which we compare with a_{th}.

Plots of experimentally obtained $AT^3\Delta T/\dot{Q}$ vs. T for several epoxy–metal sandwiches are shown in Fig. 10. The values of R_B obtained from the intercepts as explained above are shown by $(\times)$ on Fig. 7. Note that the experimental points fall very close to the predicted values, or lie at somewhat larger values of λ/l as though some phonon scattering mechanism in addition to electrons were present in the metals. We in fact attempted to increase the attenuation by sandblasting both the Cu and W surfaces with 27-μm airborne abrasive powder. Sandblasting the W surface produced no change in R_B outside the usual $\approx \pm 5\%$ irreproducibility from sample to sample. Referring to Fig. 7 one indeed should not expect much change since λ/l due to electrons is already very large. For Cu, sandblasting reduced R_B by 20%, but reannealing the surface did not restore R_B to its original value. Hence the 20% decrease probably represents the increase in effective surface area of Cu with sandblasting. Referring again to Fig. 7 one notes that R_B for a Cu–epoxy interface is very insensitive to λ/l. Hence both W and Cu were poor choices in attempting to look for the effect of surface damage, but the experiments were carried out prior to the theoretical computations.

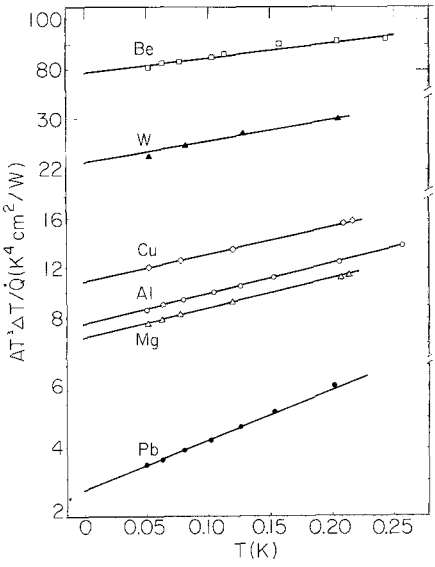

Fig. 10. Ratio of the experimental values $AT^3\Delta T/\dot{Q}$ vs. temperature T for six metal–dielectric–metal sandwiches. Note the change in the vertical scale.

A more convenient comparison of theory and experiment is presented in Fig. 11. Here the low-temperature limits a_{exp}/a_{th} are plotted vs. the acoustic impedance of the metal. Precise agreement between theory and experiment would be represented by the horizontal line. Each experimental result is compared with three theories, namely, the blackbody or radiation limit ($\bar{w} = 1$), the usual acoustic mismatch theory ($\alpha_i = 0$), and the modified acoustic mismatch theory developed in Section 2 ($\alpha_i \neq 0$). For ratios of acoustic impedances near unity, all three models give nearly the same result, and all agree rather well with experiment. But as the acoustic mismatch increases the

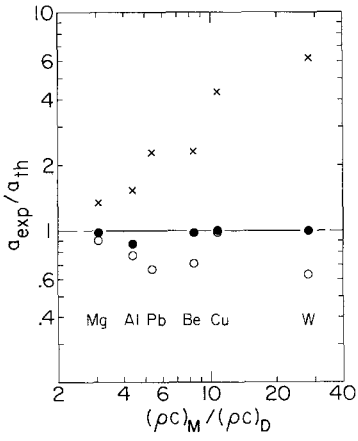

Fig. 11. The ratio a_{exp}/a_{th}, which is essentially the ratio of measured to calculated R_B at the limit of very low temperatures, vs. $(\rho c)_M/(\rho c)_D$, the ratio of the acoustic impedance of the metal to that of the dielectric. (×), calculated from the radiation or blackbody limit; (○), calculated from the acoustic mismatch theory; (●), calculated from the acoustic mismatch theory modified to include phonon attenuation caused only by electrons.

blackbody model deviates from experiment by over 600%, the acoustic mismatch model by over 30%, and the present theory by very little. Hence the present theory appears to provide a physical description of thermal transport across interfaces. Note that for W or Be roughly 30% of the boundary conductance is due to the direct interaction of phonons in the dielectric with electrons in the metal, whereas for Cu the refracted phonons account for essentially all the thermal flux.

No adjustable parameters have been used in comparing theory and experiment on solid–solid interfaces. It was necessary to make certain assumptions concerning the relative importance of attenuation of transverse and longitudinal phonons, but these assumptions have been tied to experiment or theory and have been stated explicitly.

Several previous measurements of R_B for dielectric–metal interfaces have been reported, in general for temperatures $\gtrsim 1$ K. The excellent agreement between theory and experiment for a Cu–superconducting Sn junction[49] could not be reproduced,[50] and included a factor of ≈ 3 error in the computation of R_B. Measurements between sapphire and Sn have been reviewed by Park and Narahara.[17] In general, there has been poor agreement between this type of experiment and theory. Also, with Sn in the superconducting state R_B increases somewhat relative to the normal state. This is contrary to the present theory since the sapphire has the greater acoustic velocity and any change in attenuation in the metal should have little effect on R_B. However, Cheeke has demonstrated the difficulty of measuring R_B for a metal in the superconducting state,[12] and such measurements involving a superconductor must be viewed with some suspicion. There is also the problem discussed above of ascribing a temperature to the phonon population in the sapphire[51] or the superconductor, especially since the nature of the surface scattering of phonons is not known.

Nevertheless, we have also attempted to measure R_B at a dielectric–superconductor interface. The experimental arrangement is shown by the insert in Fig. 12. On each block a tab of metal 0.05 cm thick protruded parallel to the Mylar at the interface. This free-standing tab of metal served to support a resistance thermometer and hence place it in thermal contact with the block as close to the interface as possible. The data are shown in Fig. 12 for Pb and Al; the effects of the dielectric layer have not been subtracted. The change in $AT^3\Delta T/\dot{Q}$ between the normal and superconducting states of Pb is similar to that observed by previous authors[17] and may reflect the presence of a strained layer in the Pb next to the interface which adds a thermal resistance in series with R_B.[12] For Al, however, both larger and smaller values of $AT^3\Delta T/\dot{Q}$ are observed in the superconducting state. It may be that we have not properly ascribed a temperature to phonons in the Al (or the Pb) because of the long phonon mean free path and a lack of inelastic

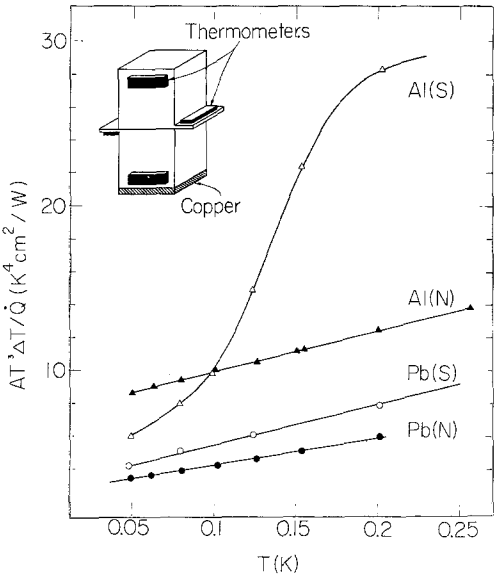

Fig. 12. Ratio of the experimental values $AT^3\Delta T/\dot{Q}$ vs. T for superconducting (S) and normal (N) sandwiches of Pb or Al. The experimental arrangement used is shown by the insert. The upper metal block was attached to a dilution refrigerator. The Cu foil on the lower metal block carried an electrical heater and provided a uniform distribution in delivering this heat to the sample.

scattering. On the other hand, it may be that the Al data reflect a resonant attenuation of phonons by dislocations at the interface and hence an enhanced transfer of energy across the interface. The resonant frequency is roughly 0.05 K or 5×10^9 Hz. This would correspond to an average dislocation loop length of $\approx 2 \times 10^{-5}$ cm,[39] a reasonable value. For a similar loop length the resonance in Pb would be about a factor of five lower in temperature. It therefore would not be observed in the present measurements. In addition, it is the attenuation in the *epoxy*, not the Pb, which should effect R_B since the sound velocity is probably greater in the epoxy than in the Pb.* However, this is speculation, one simply does not have sufficient information about the behavior of phonons *within* the superconductors to make definitive statements concerning R_B.

In addition to the dc or continuous-heat-flux measurements discussed above, several measurements of R_B on solid–solid interfaces have also been made using heat-pulse techniques.[52–54] The measurements used effective

*For this reason the Pb data cannot be compared with the present theory in Figs. 7 and 11.

temperatures ranging from ≈ 2 K up to ≈ 100 K. At temperatures up to at least ≈ 10 K these data are in much better agreement with the acoustic mismatch model than the blackbody- or radiation-limit model. It is interesting that the acoustic mismatch model remains valid at frequencies higher than 10^{12} Hz.

Often the blackbody model has been used to estimate R_B simply because the computation is trivial compared to that of the acoustic mismatch model. A *rough* value of R_B which applies to any surface may be obtained from the relation $R_{(AM)}/R_{(BB)} \approx 0.4(Z_L/Z_S)$, where $R_{(AM)}$ is the acoustic mismatch result, $R_{(BB)}$ is the blackbody result, and Z_L and Z_S are the larger and smaller acoustic impedances of the two materials. $R_{(BB)}$ and $R_{(AM)}$ set a lower and upper limit on R_B and thus bracket the actual value which would be obtained from the present theory were the phonon attenuation known.

4. SUMMARY

We have presented evidence that thermal transfer between many different materials may be understood in terms of acoustic mismatch and acoustic dissipation, ideas which have been available for many years but which have not simultaneously and systematically been directed to a solution of the thermal transfer problem. In brief, inclusion of attenuation permits the transfer of energy across an interface by phonons incident at angles greater that the acoustic critical angle. The theory contains the earlier, incomplete theoretical results of Khalatnikov, Little, and others. It is in excellent agreement with measurements on solid–solid interfaces for ratios of acoustic impedances of the two solids ranging from ≈ 3 (Mg/epoxy) to ≈ 800 (Cu/solid ^{3}He). It is also in good agreement with measurements on liquid ^{3}He and liquid ^{4}He to copper at temperatures below ≈ 0.2 K, including the small pressure dependence, the general absence of a strict T^3 temperature dependence, and the strong dependence on strain near the copper surface. At temperatures above ≈ 0.2 K an acoustic penetration depth associated with helium interfaces becomes of order of atomic dimensions, and it is not obvious if the theory should remain valid.

It is hoped that the present paper will have dissipated some of the magic previously associated with providing practical thermal contact at very low temperatures. There are, of course, other questions which remain to be answered, such as the effect of solid gas overlays on the R_B of ^{3}He–Cu interfaces,[10] the coupling of ^{3}He to paramagnetic solids,[55] and a description of additional thermal coupling mechanisms between liquid He and solids above 1 K.[56,57]

TABLE I

Values for the Various Physical Parameters Used in the Computations

Metal	Mg	Al	Pb	Cu	Be	W
ρ, g/cm^3	1.80[a]	2.73[a]	11.6[b]	9.02[a]	1.85[a]	19.3[c]
$10^{-5}c_l$, cm/sec	5.90[a]	6.79[a]	2.46[b]	4.83[a]	13.1[a]	5.25[c]
$10^{-5}c_t$, cm/sec	3.28[a]	3.24[a]	0.930[b]	2.39[a]	9.08[a]	2.91[c]
a_{exp}	6.4	7.2	2.7	11.0	77	23
$a_{(AM)}$	7.11	9.19	3.95	11.2	109	35.9
$a_{(BB)}$	4.65	4.70	1.19	2.54	33.3	3.68
$a_{(AP)}$	6.7	8.3		10.9	79	22.6
λ/l	0.044[d]	0.058[e]		0.0115[e]	0.075[d]	5.2[e]

[a]From Ref. 59.
[b]Estimated sound velocities from single-crystal data of Ref. 61.
[c]From Ref. 60.
[d]Calculated from the free-electron theory using Refs. 28, 29, and 62.
[e]Experimental values of ultrasonic attenuation—Cu,[29] W,[31] Al.[63]

APPENDIX

The theoretical values of a in Table I for the acoustic mismatch (AM), blackbody (BB), and attenuated phonon (AP) theories were found using the formula $a = (2 - \bar{w})R_B T^3$. For the attenuated phonon theory a corresponds to the value of attenuation given in the last row. For Epibond 121, $\rho = 1.22$ g/cm^2, $c_t = 1.64 \times 10^5$ cm/sec, and $c_l = 3.22 \times 10^5$ cm/sec (see Ref. 58).

For solid ^{3}He we have calculated $\rho = 0.128$ g/cm^3, $c_l = 5.8 \times 10^4$ cm/sec, and $c_t = 2.1 \times 10^4$ cm/sec from data found in Refs. 64 and 65. Fortunately, the values of $R_B T^3$ for solid ^{3}He–Cu near $\lambda/l = 1.0$ are nearly independent of these sound velocities, or in other words that curves G of Fig. 3 calculated for various solid ^{3}He velocities cross near $\lambda/l \approx 1$.

ACKNOWLEDGMENTS

The authors profited from discussions of the various ideas presented in this paper with the participants of the Europhysics Study Conference at Albe, France, during April of 1972.

REFERENCES

1. W. A. Little, *Can. J. Phys.* **37**, 334 (1959).
2. R. J. von Gutfeld, in *Physical Acoustics* (Academic Press, New York, 1968), Vol. V, p. 233.
3. W. L. Johnson and A. C. Anderson, *Phys. Letters* **37A**, 101 (1971).

4. R. E. Peterson and A. C. Anderson, *Solid State Commun.* **10**, 891 (1972).
5. R. E. Peterson and A. C. Anderson, *Phys. Letters* **40A**, 317 (1972).
6. T. H. K. Frederking, Chemical Engineering Progress Symposium Series, *Advances in Cryogenic Heat Transfer* **64**, 21 (1968).
7. G. L. Pollack, *Rev. Mod. Phys.* **41**, 48 (1969).
8. N. S. Snyder, *Cryogenics* **10**, 89 (1970); *NBS Tech. Note* 385 (1969).
9. J. D. N. Cheeke, *J. Phys. Paris*, Colloque Suppl. C3, **31**, 9 (1970).
10. A. C. Anderson and W. L. Johnson, *J. Low Temp. Phys.* **7**, 1 (1972).
11. P. L. Kapitza, *Collected Papers of P. L. Kapitza*, D. ter Haar, ed. (Pergamon Press, Oxford, 1967), Vol. II, p. 581.
12. J. D. N. Cheeke, *Cryogenics* **10**, 463 (1970).
13. A. B. Pippard, *Proceedings of the VII International Conference on Low Temperature Physics* (University of Toronto Press, Toronto, 1960), p. 476.
14. W. A. Little, *Phys. Rev.* **123**, 435 (1961).
15. R. E. Peterson, Ph.D. thesis, University of Illinois, 1972, unpublished.
16. H. Kolsky, *Stress Waves in Solids* (Oxford University Press, London, 1953).
17. B. S. Park and Y. Narahara, *J. Phys. Soc. Japan* **30**, 760 (1970).
18. R. Stoneley, *Proc. Roy. Soc.* (*London*) **A106**, 416 (1924); see also W. M. Ewing, W. S. Jardetsky, and F. Press, *Elastic Waves in Layered Media* (McGraw-Hill, New York, 1957).
19. F. L. Becker and R. L. Richardson, in *Research Techniques in Nondestructive Testing*, R. S. Sharp, ed. (Academic Press, New York, 1970), Vol. 1, p. 91, and papers cited therein.
20. F. L. Becker, *J. Appl. Phys.* **42**, 199 (1971).
21. I. M. Khalatnikov, *An Introduction to the Theory of Superfluidity* (W. A. Benjamin, New York, 1965), p. 138.
22. A. C. Anderson, J. I. Connolly, and J. C. Wheatley, *Phys. Rev.* **135**, A910 (1964); A. C. Anderson, J. I. Connolly, O. E. Vilches, and J. C. Wheatley, *Phys. Rev.* **147**, 86 (1966).
23. J. C. Wheatley, R. E. Rapp, and R. T. Johnson, *J. Low Temp. Phys.* **4**, 1 (1971).
24. I. L. Bekarevich and I. M. Khalatnikov, *Soviet Phys.—JETP* **12**, 1187 (1961).
25. J. Gavoret, *Phys. Rev.* **137**, A721 (1965).
26. I. A. Fomin, *Soviet Phys.—JETP* **27**, 1010 (1968).
27. R. Radebaugh and J. D. Siegwarth, *Proceedings of LT13*, to be published.
28. A. B. Pippard, *Phil. Mag.* **46**, 1104 (1955); *Proc. Roy. Soc.* (*London*) **A257**, 165 (1960).
29. R. E. MacFarlane and J. A. Rayne, *Phys. Rev.* **162**, 532 (1967); E. Y. Wang, R. J. Kolouch, and K. A. McCarthy, *Phys. Rev.* **175**, 723 (1968).
30. P. Lindenfeld and W. B. Pennebaker, *Phys. Rev.* **127**, 1881 (1962).
31. C. K. Jones and J. A. Rayne, *Phys. Letters* **13**, 282 (1964).
32. M. H. Jericho, *Phil. Trans. Roy. Soc.* (*London*) **A257**, 385 (1965).
33. A. F. Andreev, *Soviet Phys.—JETP* **16**, 1084 (1963).
34. L. J. Challis and J. D. N. Cheeke, *Proc. Roy. Soc. London* **304A**, 479 (1968).
35. J. K. Wigmore, *Phys. Letters* **37A**, 293 (1971).
36. A. C. Anderson and S. C. Smith, *J. Phys. Chem. Solids* **34**, 111 (1973).
37. F. R. Rollins, Jr., *Mater. Evaluation* **24**, 683 (1966).
38. H. Haug and K. Weiss, *Phys. Letters* **40A**, 19 (1972).
39. M. E. Malinowski and A. C. Anderson, *Phys. Letters* **37A**, 291 (1971); A. C. Anderson and M. E. Malinowski, *Phys. Rev.* **5B**, 3199 (1972).
40. I. M. Khalatnikov, *Zh. Eksperim. i Teor. Fiz.* **22**, 687 (1952).
41. O. Weis, *Z. Angew. Phys.* **26**, 325 (1969).
42. L. J. Challis and R. A. Sherlock, *J. Phys. C* **3**, 1193 (1970).
43. J. E. Robichaux and A. C. Anderson, *Rev. Sci. Instrum.* **40**, 1512 (1969).
44. A. C. Anderson, R. E. Peterson, and J. E. Robichaux, *Rev. Sci. Instrum.* **41**, 528 (1970).
45. A. C. Anderson, in *Temperature, Its Measurement and Control in Science and Industry* (Instrument Society of America, Pittsburgh, 1972), Vol. IV, p. 773.
46. A. C. Anderson, J. T. Folinsbee, and W. L. Johnson, *J. Low Temp. Phys.* **5**, 591 (1971).
47. K. Balcerek, J. Rafalowicz, and B. Sujak, *Acta Phys.* Polon. **32**, 935 (1967).
48. R. E. Peterson and A. C. Anderson, *Rev. Sci. Instrum.* **43**, 834 (1972); L. N. Scherr and A. C. Anderson, unpublished.

49. L. J. Barnes and J. R. Dillinger, *Phys. Rev. Letters* **10**, 287 (1963).
50. L. J. Barnes and J. R. Dillinger, *Phys. Rev.* **141**, 615 (1966).
51. D. A. Neeper and J. R. Dillinger, *Phys. Rev.* **135**, A1028 (1964).
52. P. Herth and O. Weis, *Z. Angew. Phys.* **29**, 101 (1970).
53. J. K. Wigmore, *Phys. Rev.* **5B**, 700 (1972).
54. J. D. N. Cheeke, B. Hebral, and C. Martinon, *J. de. Phys.*, to be published.
55. W. C. Black, A. C. Mota, J. C. Wheatley, J. H. Bishop, and P. M. Brewster, *J. Low Temp. Phys.* **4**, 391 (1971); J. H. Bishop, D. W. Cutter, A. C. Mota, and J. C. Wheatley, to be published.
56. C-J. Guo and H. J. Maris, *Phys. Rev. Letters* **29**, 855 (1972).
57. H. J. Trumpp, K. Lassmann, and W. Eisenmenger, *Phys. Letters* **41A**, 431 (1972).
58. A. S. Athougies, B. T. Peterson, G. L. Salinger, and C. D. Swartz, *Cryogenics* **12**, 125 (1972).
59. O. L. Anderson, in *Physical Acoustics*, W. P. Mason, ed. (Academic Press, New York, 1965), Vol. III, p. 43.
60. F. H. Featherston and J. R. Neighbors, *Phys. Rev.* **130**, 1324 (1963).
61. D. L. Waldorf, *Bull. Am. Phys. Soc.* **5**, 170 (1960).
62. American Institute of Physics Handbook, 2nd Ed. (McGraw-Hill, New York, 1963), pp. 9–4, 9–6.
63. K. C. Hepfer and J. A. Rayne, *Phys. Letters* **30A**, 281 (1969).
64. D. S. Greywall and J. A. Munarin, *Phys. Rev. Letters* **24**, 1282 (1970).
65. W. Keller, in *Helium*^{3} *and Helium*^{4} (Plenum Press, New York, 1969), p. 361.